

Supplementary Material for

Testing the sensory tradeoff hypothesis in New World bats

Jinwei Wu^{#,1}, Hengwu Jiao^{#,1}, Nancy B. Simmons², Qin Lu^{*,1}, and Huabin Zhao^{*,1}

¹Department of Ecology and Hubei Key Laboratory of Cell Homeostasis, College of Life Sciences, Wuhan University, Wuhan 430072, China

²Department of Mammalogy, American Museum of Natural History, New York 10024, United States of America

This file includes:

Supplementary background

Supplementary methods

Supplementary results

Supplementary discussion

Supplementary references

tables S1-S4

figures S1-S7

Supplementary background

About 2000 years ago, Aristotle identified the five basic senses in humans including sight (vision), hearing (audition), taste (gustation), smell (olfaction), and touch (somatosensation) [S1]. Beyond these five commonly recognized senses, additional sensory modalities may be used to detect environmental stimuli including temperature (thermoception), pain (nociception), and balance (equilibrioception). Depending on the species, animals may rely on distinct sets of sensory modalities, with some species lacking one or more basic senses while others developing novel senses [S2-4]. The absence or reduction of a sense may have been shaped by positive selection [S5], convergent evolution [S6], and sensory tradeoffs [S7]. The sensory tradeoff hypothesis has been proposed frequently in cases in which an enhancement of one sensory modality has apparently resulted in the loss or reduction of other sensory modalities, possibly due to energy limitations [S8]. For example, the loss of vomeronasal olfaction coincided with the acquisition of trichromatic color vision in primates [S9]; similarly, the origin of a novel sensory modality – high-duty-cycle (HDC) echolocation – may have resulted in the loss of color vision in some lineages of bats [S7]. Such tradeoffs have been long observed in vertebrate brain regions, with an enlargement of one region being coupled with a reduction of another [S10]. Given the finite energy budgets in animals, sensory tradeoffs have been thought to result from the high energetic demands incurred by neural processing [S8].

Among the five basic senses, the visual system is particularly prone to be lost or reduced in nocturnal, cave-dwelling, and subterranean animals [S11]. In mammals, members of at least five orders (Carnivora, Cetacea, Chiroptera, Primates, and Rodentia) have independently lost color vision [S11]. Such widespread losses have been suggested to be driven by nocturnality, spectral tuning of opsins, adaptive gene loss, and taxon-specific reasons (each taxon may have a unique scenario underlying the gene loss) [S11]. It is not surprising that taxon-specific reasons underlie the widespread losses of color vision across animals, because they have evolved

taxon-specific adaptive characteristics that have allowed them to successfully radiate in diverse ecological niches.

One group of animals that show lineage-specific loss of color vision is the mammalian order Chiroptera: the bats [S7]. We found two sister clades of Old World HDC bats (Rhinolophidae and Hipposideridae) have lost the ability to distinguish colors, while the majority of LDC bats have dichromatic color vision in our previous study [S7]. Thus, a sensory tradeoff hypothesis between the loss of color vision and the origin of the HDC echolocation in bats was proposed [S7]. However, this hypothesis between the innovation of HDC echolocation and loss of color vision may be just a mere coincidence, and additional data and analyses are needed to justify this hypothesis. One powerful approach for addressing the issue of sensory tradeoffs is to examine replicated evolution of sensory modalities in phylogenetically divergent lineages. So we turn to the New World bats, which include the moustached bats (*Pteronotus parnellii*) and vampire bats. The former have independently evolved the HDC echolocation that is similar to the hipposiderid and rhinolophid lineages [S12, 13], while the latter have evolved a unique sensory modality among bats – the infrared sense [S3, 14]. The infrared sensing ability in the common vampire bat (*Desmodus rotundus*) was first discovered by the thermography experiment [S3]. Specifically, the three pits surrounding the central nose were found to always keep a lower temperature than other areas, which can be used to detect thermal radiation of their endothermic prey and locate optimal bite sites [S3]. An additional study identified a specific nucleus on the brainstem of the common vampire bat, which may be a part of the infrared processing system of vampire bats as it resembles with the features of the infrared nucleus in infrared-sensitive snakes [S15]. Despite the infrared processing system has not yet been investigated in the other two vampire bats (*Diphylla ecaudata* and *Diaemus youngi*), similar structures were expected to be present [S14, 16].

Supplementary methods

Critical spectral tuning sites and sliding window analysis

Previous studies have identified at least 11 amino acid sites involved in the spectral tuning of SWS1 pigments [S17] and 5 amino acid sites involved in the spectral tuning of M/LWS pigments, respectively [S18]. To examine the critical spectral tuning sites of *SWS1* and *M/LWS* genes in the New World bats, we deduced the SWS1 protein sequences of the New World bats and aligned them with the house mouse (*Mus musculus*) (GenBank accession: NM_007538), and the deduced M/LWS protein sequences of the common vampire bat *Desmodus rotundus* was aligned with those of other bats published previously [S7] and that of *Homo sapiens* (GenBank accession: NM_020061). Both alignments were performed using the BioEdit program [S19].

To visualize the average rates of nonsynonymous (d_N) and synonymous (d_S) substitutions per site for sequences with ORF-disrupting indels, the Nei and Gojobori method [S20] implemented in the program SWAAP 1.0.2 [S21] was applied. The SWAAP program estimates changes of evolutionary rates with a sliding window approach. All estimations were performed using a window size of 90 nt and a step size of 9 nt, except the white-winged vampire bat *Diaemus youngi* that was estimated with a window size of 30 nt and a step size of 6 nt.

Ancestral sequence reconstruction and evolutionary analysis

Ancestral sequences were inferred with a combination of the likelihood-based method [S22] implemented in the baseml program in PAML 4.8a [S23] and maximum parsimony [S24]. Maximum parsimony was employed primarily to infer the indel regions of the ancestral sequence because the Bayesian method could not deal with the indels. To examine whether a particular lineage of bats had undergone differential selective pressures as compared to other bats, we estimated the ratio (termed ω) of nonsynonymous (d_N) to synonymous (d_S) substitution rates using branch models in codeml program implemented in PAML 4.8a [S23]. The value of ω is an indicator of natural selection, with an ω value being equal to 1, less than 1, more than 1 indicating neutral evolution, purifying selection, and positive selection, respectively [S25].

A total of six selection tests using the codeml program were undertaken in our study. First, we tested whether the intact *SWS1* genes in the 15 bats (Dataset I in **table S3**) were subjected to purifying selection (model **A0** versus model **B1** in **table S3**). Second, we tested whether there is a difference in ω between the ancestral branch of vampire bats and other branches (model **C0** and model **D2** in **table S3**). Third, we tested whether the signal of relaxed selection has occurred in *Desmodus rotundus* (model **E0** and model **F2** in **table S3**). Fourth, we tested whether the signal of relaxed selection has occurred in *Diphylla ecaudata* (model **G0** and model **H2** in **table S3**). Fifth, we tested whether the signal of relaxed selection has occurred in *Diaemus youngi* (model **I0** and model **J2** in **table S3**). Finally, we conducted the relaxed selection test towards the null allele of *Pteronotus mesoamericanus* (model **K0** and model **L2** in **table S3**).

In addition, we detected whether relaxed selection occurred using the RELAX program [S26] implemented in HyPhy [S27]. The RELAX program detects relaxed selection based on codon levels. During calculation, the selection intensity parameter (k) will be introduced to compare the test branches with the reference branches. Similar to those models used in codeml, the RELAX program compares a null model assuming k equal to 1 for all branches with an alternative model assuming a different k value in test branches. If the alternative model fits the datasets better, selective strength will be considered as relaxed ($k < 1$) or intensified ($k > 1$) in the test branches relative to reference branches. In our study, the ancestral lineage of vampire bats, *Desmodus rotundus*, *Diphylla ecaudata*, *Diaemus youngi* and *Pteronotus mesoamericanus* were used as the test branches, respectively, while the remaining branches in each case were used as reference branches. Therefore, a total of five selection tests were undertaken using RELAX in our study (**table S3**).

Dating the pseudogenization events of *SWS1*

Pseudogenization events were found in four *SWSI* sequences, including three in vampire bats, and one in the null allele of *Pteronotus mesoamericanus*, and we investigated when the functional constraint on *SWSI* became relaxed in each sequence. We assumed that the functional relaxation on *SWSI* started at t million years ago (Ma), and the pseudogenization timing was estimated based on two different methods described in Meredith et al. [S28] and Zhao et al. [S29], respectively. The first method, known as the “synonymous substitution rate method”, is based on changes in ω values (the ratio of non-synonymous to synonymous substitution rates). Specifically, the branch model in codeml [S23] was used to estimate ω for three different branch categories: functional branch, mixed branch and pseudogenic branch. The functional branches were the branches considered as background branches (those associated with the 15 New World bats with intact *SWSI*), and the mixed branch was the branch on which the relaxation of the functional constraint started. The pseudogenic branches were the branches on which the *SWSI* would be expected to evolve neutrally, thus the ω was fixed to 1 on those branches (the branches of the 4 bats possess *SWSI* pseudogenes). Except for the estimation of ω values for three branch categories, the divergence time was also needed for the estimation of t . Approximate divergence dates were taken from the following resources: (1) 27.0 Ma for the split between vampire bats (Desmodontinae) and New World fruit bats (Phyllostominae) [S30]; (2) 13.5 Ma for the divergence between *Pteronotus mesoamericanus* and *Pteronotus davyi* [S30]. The starting time (t) of functional relaxation was then obtained under the assumption of “a single rate of synonymous substitution on functional and pseudogenic branches” and “two rates of synonymous substitution on functional and pseudogenic branches”, respectively. The mean of the two values of t obtained under the two assumptions was calculated and used in our subsequent analysis. Moreover, we modified this method by bootstrapping the codons of *SWSI* 10000 times, and estimated a posterior probability distribution of t .

In the second method, t was estimated based on the number of existing ORF-disrupting mutations [S29]. This method assumes that if the observation number

of ORF-disrupting substitutions in a gene is n , the starting time (t) of functional relaxation of this gene should be between t_n and t_{n+1} by estimating the waiting times for n (t_n) and $n+1$ (t_{n+1}) ORF-disrupting substitutions. In our study, the observation number of ORF-disrupting substitutions in *SWS1* in the *Desmodus rotundus*, *Diphylla ecaudata*, *Diaemus youngi*, and *Pteronotus mesoamericanus* (the null allele) is 2, 2, 1, and 1, respectively. Waiting times were estimated using the modified program PSEUDOGENE [S9]. This program requires neutral rates of point mutations and indel mutations as input, we took both parameters from our previous study [S31]. Using the *SWS1* sequence of *Artibeus jamaicensis* as the input for the estimation of time t for the three vampire bats and the *SWS1* sequence of *Pteronotus davyi* as the input for the estimation of t for *Pteronotus mesoamericanus*, the pseudogenization process was simulated 10000 times and we acquired 10000 t for each of four species. Thus, another posterior probability distribution of t was estimated. Since independent information for the estimation of posterior probability distribution of t was used in the two methods, we combined them to obtain a final posterior probability distribution of t .

Supplementary results

Conservation of *SWS1* in most New World bats

The *SWS1* gene in mammals contains five exons and approximately 1000 nucleotides, which encode a seven-transmembrane-domain protein [S32]. By sequencing the *SWS1* gene in 16 species of New World bats, we newly obtained *SWS1* sequences spanning exon 1 to exon 4 in these species. In addition, we retrieved three additional *SWS1* sequences of New World bats from our previous study [S7]. Our dataset of *SWS1* contained all three species of vampire bats and other major lineages of the New World leaf-nosed bats (Phyllostomidae) as well as one species of New World HDC echolocating bat (Mormoopidae) (**figure 1 and table S1**). After aligning *SWS1* sequences, we found 15 of the 19 bats to have a putatively functional *SWS1* gene characterized by an intact open reading frames (ORFs) (**figure 1**). The deduced protein sequences of these intact genes were subsequently aligned and used to

examine whether the 11 critical sites responsible for the spectral tuning are conserved in these species. The alignment (**figure S6**) showed that these functionally critical sites in each species are identical to those in the mouse (*Mus musculus*), which is known to have an ultraviolet (UV) pigment conferred by the SWS1 opsin [S33]. Of note, all the 15 bats with an intact and putative functional SWS1 opsin are low-duty-cycle (LDC) echolocators [S12]. **We note that an intact *SWS1* can not predict dichromatic color vision in a bat, as functional loss of a gene may have occurred at transcriptional or translational stage.**

To examine whether these 15 intact *SWS1* genes are under purifying selection and functional constraint, we undertook a selection test on bats by estimating the ratio (termed ω) of nonsynonymous (d_N) to synonymous (d_S) substitution rates. In this test, we assumed a uniform ω across all branches (model **A0** in **table S3**), and the value of ω was estimated to be 0.16. The model A was next compared with the model **B1**, which assumed all branches have a same $\omega = 1$ (**table S3**). This comparison revealed a significant difference between the two models, suggesting the overall ω of all intact genes is significantly smaller than 1 ($\omega = 0.16$, $P = 1.70E-51$, **table S3**). Thus, the *SWS1* gene is under overall strong purifying selection and functional constraint in these bats. We additionally examined overall variation of *SWS1* across all 15 bats with intact ORFs by comparing the gene tree with species tree. Both maximum-likelihood and Bayesian approaches recovered a same tree topology (**figure S7**), which is not significantly different from the species tree [S30, 34, 35] (Kishino–Hasegawa test, $P = 0.181$; Shimodaria–Hasegawa test, $P = 0.169$; **table S4**). This comparison suggests that the overall variation of the intact *SWS1* sequences across these bats is low, confirming the conservation of *SWS1* in these species.

Supplementary discussion

In this work, we used New World bats to test the sensory tradeoff hypothesis between a loss of color vision and an origin of high-duty-cycle (HDC) echolocation [S7]. Through sequencing the short-wavelength opsin gene (*SWS1*) in 16 species (29

individuals) of New World bats, we found losses of color vision in the New World HDC echolocators, the same sensory tradeoff in Old World bats was replicated in New World bats. In addition, *SWS1* was found to be pseudogenized in all three vampire bats, suggesting another sensory tradeoff between the gain of the infrared sense in vampire bats and the loss of color vision.

In contrast to the pseudogenization of *SWS1* gene in the four New World bats (one HDC echolocator and three vampire bats), the *SWS1* opsin gene appears to be evolutionarily conserved in most New World bats examined (**figures 1 and S6a**). The 11 critical sites implicated in spectral tuning are identical in all species with an intact *SWS1* gene (**figure S6a**), which is predicted to encode a UV sensitive pigment [S17]. Indeed, behavioral studies have showed that eight species of New World bats are able to perceive UV visual stimuli [S36, 37], including one species of New World leaf-nosed bat (*Glossophaga soricina*) that was examined in this study [S36] (**figure 1**). Genetic evidence indicates that most bats, including New World and Old World species, possess UV color vision [S7], and a behavioral study confirmed the cone-based UV sensitivity in two Old World bats [S38]. Why is UV vision retained in most bats? Potential benefits of UV vision in bats and other mammals include the detection of UV-reflective foods (e.g. flowers, fruits, and insects) or urine marks, communication with potential mates, and entrainment of circadian rhythms [S7, 36, 39, 40]. Nonetheless, the selective forces underlying the retention of UV vision in bats remain unclear.

Color vision in eutherian mammals is conferred by M/LWS and SWS1 opsins [S11]. The *M/LWS* opsin gene displays strong conservation and no ORF-disruptive mutations are known in mammals with the exception of a few cetacean species [S7, 41, 42]. Even in the highly specialized vampire bats, we observed intact ORFs and highly conserved protein sequences, through sequencing all six exons (≈ 1300 bp) of the *M/LWS* gene in five individuals of the common vampire bat (**figure S6b**). Thus, the disruption or pseudogenization of the *M/LWS* gene may represent a fitness damage

that most mammals cannot tolerate, suggesting an indispensable role in certain physiological needs such as the regulation of circadian rhythms [S41], **although it remains to be tested whether the gene is functional at transcriptional or translational stage.**

Supplementary references

- S1. Sorabji, R. 1971 Aristotle on demarcating the five senses. *Philos. Rev.* **80**, 55-79. (doi:10.2307/2184311)
- S2. Au, W.W.L. & Simmons, J.A. 2007 Echolocation in dolphins and bats. *Physics Today* **60**, 40.
- S3. Kurten, L. & Schmidt, U. 1982 Thermoperception in the common vampire bat (*Desmodus rotundus*). *J. Comp. Physiol. A* **146**, 223-228. (doi:doi.org/10.1007/BF00610241)
- S4. Feng, P., Zheng, J., Rossiter, S.J., Wang, D. & Zhao, H. 2014 Massive losses of taste receptor genes in toothed and baleen whales. *Genome Biol. Evol.* **6**, 1254-1265. (doi:10.1093/gbe/evu095)
- S5. David-Gray, Z.K., Janssen, J.W., DeGrip, W.J., Nevo, E. & Foster, R.G. 1998 Light detection in a 'blind' mammal. *Nat. Neurosci.* **1**, 655-656. (doi:10.1038/3656)
- S6. Wilkens, H. & Strecker, U. 2003 Convergent evolution of the cavefish *Astyanax* (Characidae, Teleostei): genetic evidence from reduced eye-size and pigmentation. *Biol. J. Linn. Soc.* **80**, 545-554. (doi:10.1111/j.1095-8312.2003.00230.x)
- S7. Zhao, H., Rossiter, S.J., Teeling, E.C., Li, C.J., Cotton, J.A. & Zhang, S. 2009 The evolution of color vision in nocturnal mammals. *Proc. Natl Acad. Sci. USA.* **106**, 8980-8985. (doi:10.1073/pnas.0813201106)
- S8. Niven, J.E. & Laughlin, S.B. 2008 Energy limitation as a selective pressure on the evolution of sensory systems. *J. Exp. Biol.* **211**, 1792. (doi:10.1242/jeb.017574)
- S9. Zhang, J. & Webb, D.M. 2003 Evolutionary deterioration of the vomeronasal pheromone transduction pathway in catarrhine primates. *Proc. Natl Acad. Sci. USA.* **100**, 8337-8341. (doi:10.1073/pnas.1331721100)
- S10. Harvey, P.H. & Krebs, J.R. 1990 Comparing brains. *Science* **249**, 140-146. (doi:10.1126/science.2196673)
- S11. Jacobs, G.H. 2013 Losses of functional opsin genes, short-wavelength cone photopigments, and color vision—a significant trend in the evolution of mammalian vision. *Visual Neurosci.* **30**, 39-53. (doi:10.1017/S0952523812000429)
- S12. Jones, G. & Teeling, E.C. 2006 The evolution of echolocation in bats. *Trends Ecol. Evol.* **21**, 149-156. (doi:https://doi.org/10.1016/j.tree.2006.01.001)
- S13. Arita, H.T. & Fenton, M.B. 1997 Flight and echolocation in the ecology and evolution of bats. *Trends Ecol. Evol.* **12**, 53-58.

- (doi:10.1016/S0169-5347(96)10058-6)
- S14. Altringham, J.D. & Fenton, M.B. 2003 *Bat ecology*. Chicago, University of Chicago Press.
- S15. Kishida, R., Goris, R.C., Terashima, S.-I. & Dubbeldam, J.L. 1984 A suspected infrared-recipient nucleus in the brainstem of the vampire bat, *Desmodus rotundus*. *Brain Res.* **322**, 351-355. (doi:10.1016/0006-8993(84)90132-x)
- S16. Jones, G., Teeling, E.C. & Rossiter, S.J. 2013 From the ultrasonic to the infrared: molecular evolution and the sensory biology of bats. *Front. Physiol.* **4**, 117. (doi:10.3389/Fphys.2013.00117)
- S17. Yokoyama, S., Starmer, W.T., Takahashi, Y. & Tada, T. 2006 Tertiary structure and spectral tuning of UV and violet pigments in vertebrates. *Gene* **365**, 95-103. (doi:10.1016/j.gene.2005.09.028)
- S18. Yokoyama, S. & Radlwimmer, F.B. 1999 The molecular genetics of red and green color vision in mammals. *Genetics* **153**, 919-932.
- S19. Hall, T.A. 1999 BioEdit: a user-friendly biological sequence alignment editor and analysis program for Windows 95/98/NT. *Nucleic acids symposium series* **41**, 95-98.
- S20. Nei, M. & Gojobori, T. 1986 Simple methods for estimating the numbers of synonymous and nonsynonymous nucleotide substitutions. *Mol. Biol. Evol.* **3**, 418-426. (doi:10.1093/oxfordjournals.molbev.a040410)
- S21. Pride, D. 2004 SWAAP 1.0.2: a tool for analyzing substitutions and similarity in multiple alignments. [<http://www.bacteriamuseum.org/SWAAP/SwapPage.htm>].
- S22. Yang, Z., Kumar, S. & Nei, M. 1995 A new method of inference of ancestral nucleotide and amino acid sequences. *Genetics* **141**, 1641-1650.
- S23. Yang, Z. 2007 PAML 4: phylogenetic analysis by maximum likelihood. *Mol. Biol. Evol.* **24**, 1586-1591. (doi:10.1093/molbev/msm088)
- S24. Zhang, J. & Nei, M. 1997 Accuracies of ancestral amino acid sequences inferred by the parsimony, likelihood, and distance methods. *J. Mol. Evol.* **44**, S139-S146. (doi:10.1007/PI00000067)
- S25. Zhang, J., Nielsen, R. & Yang, Z. 2005 Evaluation of an improved branch-site likelihood method for detecting positive selection at the molecular level. *Mol. Biol. Evol.* **22**, 2472-2479. (doi:10.1093/molbev/msi237)
- S26. Wertheim, J.O., Murrell, B., Smith, M.D., Pond, S.L.K. & Scheffler, K. 2015 RELAX: detecting relaxed selection in a phylogenetic framework. *Mol. Biol. Evol.* **32**, 820-832. (doi:10.1093/molbev/msu400)
- S27. Pond, S.L.K., Frost, S.D.W. & Muse, S.V. 2005 HyPhy: hypothesis testing using phylogenies. *Bioinformatics* **21**, 676-679. (doi:10.1093/bioinformatics/bti079)
- S28. Meredith, R.W., Gatesy, J., Murphy, W.J., Ryder, O.A. & Springer, M.S. 2009 Molecular decay of the tooth gene enamelin (*ENAM*) mirrors the loss of enamel in the fossil record of placental mammals. *PLoS Genet.* **5**, e1000634. (doi:10.1371/journal.pgen.1000634)

- S29. Zhao, H., Yang, J.-R., Xu, H. & Zhang, J. 2010 Pseudogenization of the umami taste receptor gene *Tas1r1* in the giant panda coincided with its dietary switch to bamboo. *Mol. Biol. Evol.* **27**, 2669-2673. (doi:10.1093/molbev/msq153)
- S30. Rojas, D., Warsi, O.M. & Davalos, L.M. 2016 Bats (Chiroptera: Noctilionoidea) challenge a recent origin of extant neotropical diversity. *Syst. Biol.* **65**, 432-448. (doi:10.1093/sysbio/syw011)
- S31. Zhao, H., Zhou, Y., Pinto, C.M., Charles-Dominique, P., Galindo-Gonzalez, J., Zhang, S. & Zhang, J. 2010 Evolution of the sweet taste receptor gene *Tas1r2* in bats. *Mol. Biol. Evol.* **27**, 2642-2650. (doi:10.1093/molbev/msq152)
- S32. Yokoyama, S. 2000 Molecular evolution of vertebrate visual pigments. *Prog. Ret. Eye Res.* **19**, 385-419. (doi:10.1016/S1350-9462(00)00002-1)
- S33. Lyubarsky, A.L., Falsini, B., Pennesi, M.E., Valentini, P. & Pugh, E.N. 1999 UV- and midwave-sensitive cone-driven retinal responses of the mouse: A possible phenotype for coexpression of cone photopigments. *J. Neurosci.* **19**, 442-455.
- S34. Dávalos, L.M., Cirranello, A.L., Geisler, J.H. & Simmons, N.B. 2012 Understanding phylogenetic incongruence: lessons from phyllostomid bats. *Biological Reviews* **87**, 991-1024. (doi:10.1111/j.1469-185x.2012.00240.x)
- S35. Datzmann, T., von Helversen, O. & Mayer, F. 2010 Evolution of nectarivory in phyllostomid bats (Phyllostomidae Gray, 1825, Chiroptera: Mammalia). *BMC Evol. Biol.* **10**. (doi:10.1186/1471-2148-10-165)
- S36. Winter, Y., Lopez, J. & von Helversen, O. 2003 Ultraviolet vision in a bat. *Nature* **425**, 612-614. (doi:10.1038/nature01971)
- S37. Marcos Gorresen, P., Cryan, P.M., Dalton, D.C., Wolf, S. & Bonaccorso, F.J. 2015 Ultraviolet vision may be widespread in bats. *Acta Chiropte.* **17**, 193-198. (doi:10.3161/15081109ACC2015.17.1.017)
- S38. Xuan, F., Hu, K., Zhu, T., Paul, R., Wang, X. & Sun, Y. 2012 Behavioral evidence for cone-based ultraviolet vision in divergent bat species and implications for its evolution. *Zoologia (Curitiba)* **29**, 109-114. (doi:10.1590/s1984-46702012000200002)
- S39. Zhao, H., Xu, D., Zhou, Y., Flanders, J. & Zhang, S. 2009 Evolution of opsin genes reveals a functional role of vision in the echolocating little brown bat (*Myotis lucifugus*). *Biochem. Syst. Ecol.* **37**, 154-161. (doi:10.1016/j.bse.2009.03.001)
- S40. Jacobs, G.H. 1992 Ultraviolet vision in vertebrates. *Am. Zool.* **32**, 544-554. (doi:10.1093/icb/32.4.544)
- S41. Nei, M., Zhang, J. & Yokoyama, S. 1997 Color vision of ancestral organisms of higher primates. *Mol. Biol. Evol.* **14**, 611-618. (doi:10.1093/oxfordjournals.molbev.a025800)
- S42. Meredith, R.W., Gatesy, J., Emerling, C.A., York, V.M. & Springer, M.S. 2013 Rod monochromacy and the coevolution of cetacean retinal opsins. *PLoS Genet.* **9**, e1003432. (doi:10.1371/journal.pgen.1003432)

Table S1. Species and individuals used in this study.

Classification		Common name	Scientific name	AMNH sample ID	
Family	Subfamily				
Mormoopidae		Parnell's mustached bat	<i>Pteronotus mesoamericanus</i>	274564	
				274565	
				278269	
				278117	
				278393	
				278658	
		Davy's naked-backed bat	<i>Pteronotus davyi</i>	274571	
				274572	
				278293	
				278290	
				278397	
				278121	
				103067	
				278102	
Phyllostomatidae	Stenodermatinae	little yellow-shouldered bat	<i>Sturnira lilium</i>	278121	
		Cuban fig-eating bat	<i>Phyllops falcatus</i>	103067	
		tent-making bat	<i>Uroderma bilobatum</i>	278102	
		MacConnell's bat	<i>Mesophylla macconnelli</i>	109688	
	Glossophaginae	tailed tailless bat	<i>Anoura caudifer</i>	109578	
		Pallas's long-tongued bat	<i>Glossophaga soricina</i>	278304	
		Antillean fruit-eating bat	<i>Brachyphylla cavernarum</i>	121988	
		Cuban flower bat	<i>Phyllonycteris obtusa</i>	138092	
		Phyllostominae	Linnaeus's false vampire bat	<i>Vampyrum spectrum</i>	110477
			white-throated round-eared bat	<i>Lophostoma silvicolum</i>	109530
	fringe-lipped bat	<i>Trachops cirrhosus</i>	207853		

Desmodontinae	common vampire bat	<i>Desmodus rotundus</i>	278264
			278277
			278291
			278296
			278298
	white-winged vampire bat	<i>Diaemus youngi</i>	110377
	hairy-legged vampire bat	<i>Diphylla ecaudata</i>	109328

Table S2. Details of primers used in this study.

Species	Primer sequence	Product	Primer sequence	Product
<i>Sturnira lilium</i>	F: TGGGATGGGCCTCAGTACCACAT	Exon1-Exon3 of <i>SWSI</i>	F: GCAGTGTTCCTGTGGYCCYACTGGTAC	Exon3-Exon4 of <i>SWSI</i>
	R: GGCACGATGAAGCAGAAGATGAAGAGG	(≈1200bp)	R: GGAAGTCTTATTCATGAAGCAGTAGATGATGGG	(≈800bp)
<i>Phyllops falcatus</i>	F: TGAGCAARATGTCRGGGGAGGAGG	Exon1-Exon3 of <i>SWSI</i>	F: GCAGTGTTCCTGTGGYCCYACTGGTAC	Exon3-Exon4 of <i>SWSI</i>
	R: TGGTGCCACRGTGTACCAGTC	(≈1200bp)	R: GGAAGTCTTATTCATGAAGCAGTAGATGATGGG	(≈800bp)
<i>Uroderma bilobatum</i>	F: TGAGCAARATGTCRGGGGAGGAGG	Exon1-Exon3 of <i>SWSI</i>	F: GCAGTGTTCCTGTGGYCCYACTGGTAC	Exon3-Exon4 of <i>SWSI</i>
	R: TGGTGCCACRGTGTACCAGTC	(≈1200bp)	R: GGAAGTCTTATTCATGAAGCAGTAGATGATGGG	(≈800bp)
<i>Mesophylla macconnelli</i>	F: TGAGCAARATGTCRGGGGAGGAGG	Exon1-Exon3 of <i>SWSI</i>	F: GCAGTGTTCCTGTGGYCCYACTGGTAC	Exon3-Exon4 of <i>SWSI</i>
	R: TGGTGCCACRGTGTACCAGTC	(≈1200bp)	R: GGAAGTCTTATTCATGAAGCAGTAGATGATGGG	(≈800bp)
<i>Anoura caudifer</i>	F: TGAGCAARATGTCRGGGGAGGAGG	Exon1-Exon3 of <i>SWSI</i>	F: GCAGTGTTCCTGTGGYCCYACTGGTAC	Exon3-Exon4 of <i>SWSI</i>
	R: TGGTGCCACRGTGTACCAGTC	(≈1200bp)	R: GGAAGTCTTATTCATGAAGCAGTAGATGATGGG	(≈800bp)
<i>Glossophaga soricina</i>	F: TGAGCAARATGTCRGGGGAGGAGG	Exon1-Exon3 of <i>SWSI</i>	F: GCAGTGTTCCTGTGGYCCYACTGGTAC	Exon3-Exon4 of <i>SWSI</i>
	R: TGGTGCCACRGTGTACCAGTC	(≈1200bp)	R: GGAAGTCTTATTCATGAAGCAGTAGATGATGGG	(≈800bp)
<i>Brachyphylla cavernarum</i>	F: TGAGCAARATGTCRGGGGAGGAGG	Exon1-Exon3 of <i>SWSI</i>	F: GCAGTGTTCCTGTGGYCCYACTGGTAC	Exon3-Exon4 of <i>SWSI</i>
	R: TGGTGCCACRGTGTACCAGTC	(≈1200bp)	R: GGAAGTCTTATTCATGAAGCAGTAGATGATGGG	(≈800bp)
<i>Phyllonycteris obtusa</i>	F: TGAGCAARATGTCRGGGGAGGAGG	Exon1-Exon3 of <i>SWSI</i>	F: GCAGTGTTCCTGTGGYCCYACTGGTAC	Exon3-Exon4 of <i>SWSI</i>
	R: TGGTGCCACRGTGTACCAGTC	(≈1200bp)	R: GGAAGTCTTATTCATGAAGCAGTAGATGATGGG	(≈800bp)
<i>Vampyrum spectrum</i>	F: TGAGCAARATGTCRGGGGAGGAGG	Exon1-Exon3 of <i>SWSI</i>	F: GCAGTGTTCCTGTGGYCCYACTGGTAC	Exon3-Exon4 of <i>SWSI</i>
	R: TGGTGCCACRGTGTACCAGTC	(≈1200bp)	R: GGAAGTCTTATTCATGAAGCAGTAGATGATGGG	(≈800bp)
<i>Lophostoma silvicolum</i>	F: TGGGATGGGCCTCAGTACCACAT	Exon1-Exon3 of <i>SWSI</i>	F: GCAGTGTTCCTGTGGYCCYACTGGTAC	Exon3-Exon4 of <i>SWSI</i>
	R: GGCACGATGAAGCAGAAGATGAAGAGG	(≈1200bp)	R: GGAAGTCTTATTCATGAAGCAGTAGATGATGGG	(≈800bp)
<i>Trachops cirrhosus</i>	F: ATGTCAGRGGARGAGTTTTATCTGTTCAAG	Exon1-Exon3 of <i>SWSI</i>	F: GCAGTGTTCCTGTGGYCCYACTGGTAC	Exon3-Exon4 of <i>SWSI</i>
	R: TATAGKACTCGCTGCGRTAYTTGGTGCC	(≈1200bp)	R: GGAAGTCTTATTCATGAAGCAGTAGATGATGGG	(≈800bp)
<i>Desmodus rotundus</i>	F: TCAGGGAACCCAAAAGTGGCTTTG	Exon1-Exon5 of <i>SWSI</i>		
	R: GGTAGGAAGGTAATAGGAAAACGG	(≈3200bp)		

<i>Diaemus youngi</i>			F: CCRACTGGTACACTGTGGGCACC	Exon3-Exon4 of <i>SWS1</i>
			R: TGGGGTTGTAGACACAAGCACTC	(≈800bp)
<i>Diphylla ecaudata</i>	F: TCAGGGAACCCAAAAGTGGCTTTG	Exon1-Exon3 of <i>SWS1</i>	F: CACCTGGTTCCTCTTCATCTTCT	Exon3-Exon4 of <i>SWS1</i>
	R: CAGCATAGGGCACGTAACAGAGA	(≈1200bp)	R: GGTAGGAAGGTAATAGAAAACGG	(≈800bp)
<i>Pteronotus davyi</i>	F: GGTCCAGACTCTTTGAGCCC	Exon1-Exon3 of <i>SWS1</i>		
	R: TGGGGCCAACCTGGCTAGAAG	(≈3200bp)		
<i>Pteronotus mesoamericanus</i>	F: TGAGCAARATGTCRGGGGAGGAGG	Exon1-Exon3 of <i>SWS1</i>	F: GCAGTGTTCCTGTGGYCCYGACTGGTAC	Exon3-Exon4 of <i>SWS1</i>
	R: TGGTGCCACRGTGTACCAGTC	(≈1200bp)	R: GGAAGTCTTATTCATGAAGCAGTAGATGATGGG	(≈800bp)
<i>Desmodus rotundus</i>	F: CTGGACAGTAGAAGGGAACG	Exon1 of <i>LWS1</i>	F: GGAGCCTGTCAATGGCACTA	Exon2 of <i>LWS1</i>
	R: GTGACCTAAGCCCTCTCTCG	(≈1000bp)	R: CCCAGGTCCTCCTATCTTA	(≈1900bp)
<i>Desmodus rotundus</i>	F: GAATGTCCGCCACCTCTGTA	Exon3- Exon4 of <i>LWS1</i>	F: CTCCTTGTTGCCCCATACTC	Exon5 of <i>LWS1</i>
	G: GCAGGTTTCATTTGAGCGTC	(≈1900bp)	R: ATGGGCAGTTTGCTGTGGAG	(≈1100bp)
<i>Desmodus rotundus</i>	F: GCTGTTCCCTGGTTTGTAGA	Exon6 of <i>LWS1</i>		
	R: GCTCTCCGCTCTAAATCCTT	(≈900bp)		

Table S3. Tests of selective pressures on the *SWS1* gene in the New World bats.

Selective pressures tests using codeml						
Models	ω (d_N/d_S)	lnL	Δnp	Models compared	$2\Delta lnL$	<i>P</i> value
Dataset I: 15 sequences (all bats with intact <i>SWS1</i>)						
A0. All branches have the same ω	$\omega = 0.16$	-2629.38				
B1a. All branches have the same $\omega = 1$	$\omega = 1$	-2743.34	1	B vs. A	227.92	1.70E-51
Dataset II: 16 sequences (Dataset I plus the ancestral sequence of vampire bats)						
C0. All branches have the same ω	$\omega = 0.16$	-2591.66				
D2. Ancestral branch of vampire bats has ω_1 and other branches have ω_0	$\omega_0 = 0.16, \omega_1 = 1.27$	-2591.66	1	D vs. C	0	1
Dataset III: 16 sequences (Dataset I plus the <i>D. rotundus</i>)						
E0. All branches have the same ω	$\omega = 0.18$	-2924.35				
F2. <i>D. rotundus</i> has ω_1 and other branches have ω_0	$\omega_0 = 0.16, \omega_1 = 0.61$	-2918.85	1	F vs. E	11	0.00091
Dataset IV: 16 sequences (Dataset I plus the <i>D. ecaudata</i>)						
G0. All branches have the same ω	$\omega = 0.16$	-2889.69				
H2. <i>D. ecaudata</i> has ω_1 and other branches have ω_0	$\omega_0 = 0.15, \omega_1 = 0.32$	-2888.67	1	H vs. G	2.04	0.15
Dataset V: 16 sequences (Dataset I plus the <i>D. youngi</i>)						
I0. All branches have the same ω	$\omega = 0.17$	-2646.35				
J2. <i>D. youngi</i> has ω_1 and other branches have ω_0	$\omega_0 = 0.16, \omega_1 = 1.10$	-2641.64	1	I vs. J	9.42	0.0021
Dataset VI: 16 sequences (Dataset I plus the null allele of <i>P. mesoamericanus</i>)						
K0. All branches have the same ω	$\omega = 0.16$	-2652.26				
L2. <i>P. mesoamericanus</i> has ω_1 and other branches have ω_0	$\omega_0 = 0.15, \omega_1 = 0.55$	-2650.36	1	L vs. K	3.80	0.05
Selective pressures tests using RELAX						
Models	k (selection intensity)	lnL	Δnp	Models compared	$2\Delta lnL$	<i>P</i> value
Dataset II: 16 sequences (Dataset I plus the ancestral sequence of vampire bats)						
M. All branches have the same $k = 1$		-2545.94				

N. Ancestral branch of vampire bats has a different k value relative to reference branches	$k = 1.128$	-2545.94	1	N vs. M	0	1
Dataset III:16 sequences (Dataset I plus the <i>D. rotundus</i>)						
O. All branches have the same $k = 1$		-2872.23				
P. <i>D. rotundus</i> has a different k value relative to reference branches	$k = 0.197$	-2866.80	1	P vs. O	10.86	0.00098
Dataset IV:16 sequences (Dataset I plus the <i>D. ecaudata</i>)						
Q. All branches have the same $k = 1$		-2844.93				
R. <i>D. ecaudata</i> has a different k value relative to reference branches	$k = 0.545$	-2843.88	1	R vs. Q	2.10	0.147
Dataset V:16 sequences (Dataset I plus the <i>D. youngi</i>)						
S. All branches have the same $k = 1$		-2595.52				
T. <i>D. youngi</i> has a different k value relative to reference branches	$k = 0$	-2590.92	1	T vs. S	9.20	0.0024
Dataset VI:16 sequences (Dataset I plus the null allele of <i>P. mesoamericanus</i>)						
U. All branches have the same $k = 1$		-2627.51				
V. <i>P. mesoamericanus</i> has a different k value relative to reference branches	$k = 0.240$	-2625.75	1	U vs. V	3.52	0.060

Table S4. Gene vs. species tree for the *SWS1* gene in the New World bats.

Test	Log likelihood score	Difference	<i>P</i> value for KH test	<i>P</i> value for SH test
Gene tree	-3108.66			
Species tree	-3084.37	24.29	0.181	0.169

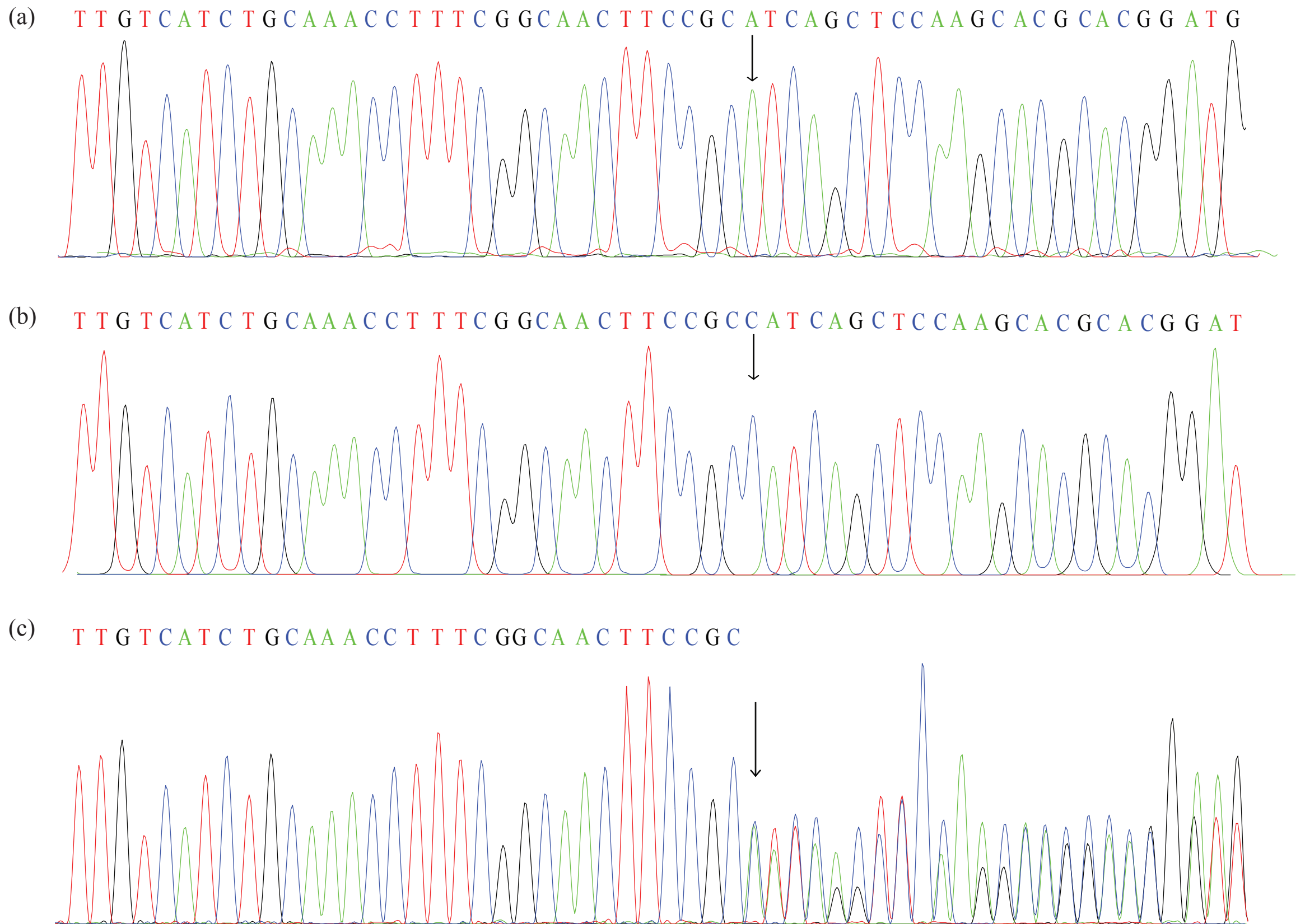


Figure S1. Sequencing chromatograms of the *SWS1* gene for *Pteronotus mesoamericanus*.

The arrow indicates the position where the 1-bp insertion occurs. (A) The intact allele cloned and sequenced;

(B) The null-allele cloned and sequenced; (C) The 1-bp insertion in the heterozygous state confirmed by direct sequencing.

	TM4										519
<i>Homo sapiens</i>	GGCAACTTCC	GC-TTCAGCT	CCAAGCATGC	ACTGACGGTG	GTCCTGGCTA	CCTGGACCAT	TGGTATTGGC	GTCTCCATCC	CACCCTTCTT	TGGCTGGAGC	
<i>Pteronotus davyi</i>	GGCAACTTCC	GC-TTCAGCT	CCAAGCACGC	GCTGATGGTA	GTCCTGGCCA	CCTGGACCAT	TGGTGTGGGC	GTCTCCATCC	CACCCTTCTT	TGGCTGGAGC	
<i>P. mesoamericanus</i> (intact allele)	GGCAACTTCC	GC-ATCAGCT	CCAAGCACGC	ACGGATGGTA	GTCCTGGCCA	CCTGGACCAT	TGGTATCGGC	GTCTCCATCC	CACCCTTCTT	TGGCTGGAGC	
<i>P. mesoamericanus</i> (null allele)	GGCAACTTCC	GC CAT CAGCT	CCAAGCACGC	ACGGATGGTA	GTCCTGGCCA	CCTGGACCAT	TGGTATCGGC	GTCTCCATCC	CACCCTTCTT	TGGCTGGAGC	
											TM5
	CGGTTTCATCC	CTGAGGGCCT	GCAGTGTTC	TGTGGCCCTG	ACTGGTACAC	CGTGGGCACC	AAATACCGCA	GCGAGTCCTA	TACGTGGTTC	CTCTTCATCT	619
	CGGTTTCATCC	CTGAAGGCCT	GCAATGTTCC	TGTGGCCCTG	ACTGGTACAC	CGTGGGCACC	AAATACCGCA	GCGAGTACTA	TACCTGGTTC	CTCTTCATCT	
	CGGTTTCATCC	CCGAAGGCCT	GCAATGTTCC	TGTGGTCCTG	ACTGGTACAC	TGTGGGCACC	AAATATCACA	GCGAGTACTA	TACCTGGTTC	CTCTTCATCT	
	CGGTTTCATCC	CCGAAGGCCT	GCAATGTTCC	TGTGGTCC TG A	ACTGGTACAC	CGTGGGCACC	AAATATCACA	GCGAGTACTA	TACCTGGTTC	CTCTTCATCT	
											719
	TCTGCTTCAT	TGTGCCTCTC	TCCCTCATCT	GCTTCTCCTA	CACTCAGCTG	CTGAGGGCCC	TGAAAGCTGT	TGCAGCTCAG	CAGCAGGAGT	CAGCTACGAC	
	TCTGCTTCAT	CGTGCCTCTT	TCCCTCATCT	GCTTCTGCTA	CTCTCAGCTG	CTGCGGGCGC	TCAGGGCTGT	TGCAGCCCAG	CAGCAGGAGT	CAGCTTCCAC	
	TCTGCTTCAT	CGTGCCTCTT	TCCCTCATCT	GCTTCTGCTA	CTCTCAGCTG	CTGCGGGCGC	TCAGGGCTGT	TGCAGCCCAG	CAGCAGGAGT	CAGCTTCCAC	
	TCTGCTTCAT	CGTGCCTCTT	TCCCTCATCT	GCTTCTGCTA	CTCTCAGCTG	CTGCGGGCGC	TCAGGGCTGT	TGCAGCCCAG	CAGCAGGAGT	CAGCTTCCAC	
											TM6
	CCAGAAGGCT	GAACGGGAGG	TGAGCCGCAT	GGTGGTTGTG	ATGGTAGGAT	CCTTCTGTGT	CTGCTACGTG	CCCTACGCGG	CCTTCGCCAT	GTACATGGTC	819
	CCAGAAGGCT	GAGCGGGAGG	TGAGCCGCGT	GGTGGTGGTG	ATGGTGGGCT	CCTTCTGTCT	CTGCTACGTG	CCCTATGCTG	CCCTGGCCAT	GTATATGGTC	
	CCAGAAGGCT	GAGCGGGAGG	TGAGCCGCAT	GGTGGTGGCG	ATGGTGGGAT	CCTTCTGTCT	CTGTTACGTG	CCCTATGCTG	CCCTGGCCAT	GTATATGGTC	
	CCAGAAGGCT	TGA GCGGGAGG	TGAGCCGCAT	GGTGGTGGCG	ATGGTGGGAT	CCTTCTGTCT	CTGTTACGTG	CCCTATGCTG	CCCTGGCCAT	GTATATGGTC	
											TM7
	AACAACCGTA	ACCATGGGCT	GGACTTACGG	CTTGTCACCA	TTCCTTCATT	CTTCTCCAAG	AGTGCTTGCA	TCTACAA			896
	AACCGCCGTA	ACCACGGGCT	GGACTTGC GG	CTTGTCACCA	TTCCTGCCTT	CTTCTCCAAG	AGCTCTTGCG	TCTACAA			
	AACAACCGTA	ACCATGGGCT	GGACTTGCAG	CTCGTCACCA	TTCCTGCCTT	CTTCTCCAAG	AGCTCTTGCG	TCTACAA			
	AACAACCGT A A	ACCATGGGCT	GGACTTGCAG	CTCGTCACCA	TTCCTGCCTT	CTTCTCCAAG	AGCTCTTGCG	TCTACAA			

Figure S2. Detailed alignment of *SWS1* sequences from *Pteronotus* species.

The 1-bp insertion and premature stop codons are boxed. Dashes are alignment gaps, question marks represent unamplified nucleotides, and numbers in the right indicate nucleotide positions following the reference sequence (*Homo sapiens*). Regions corresponding to transmembrane domains are indicated. Species indicated in bold font are high-duty-cycle echolocators.

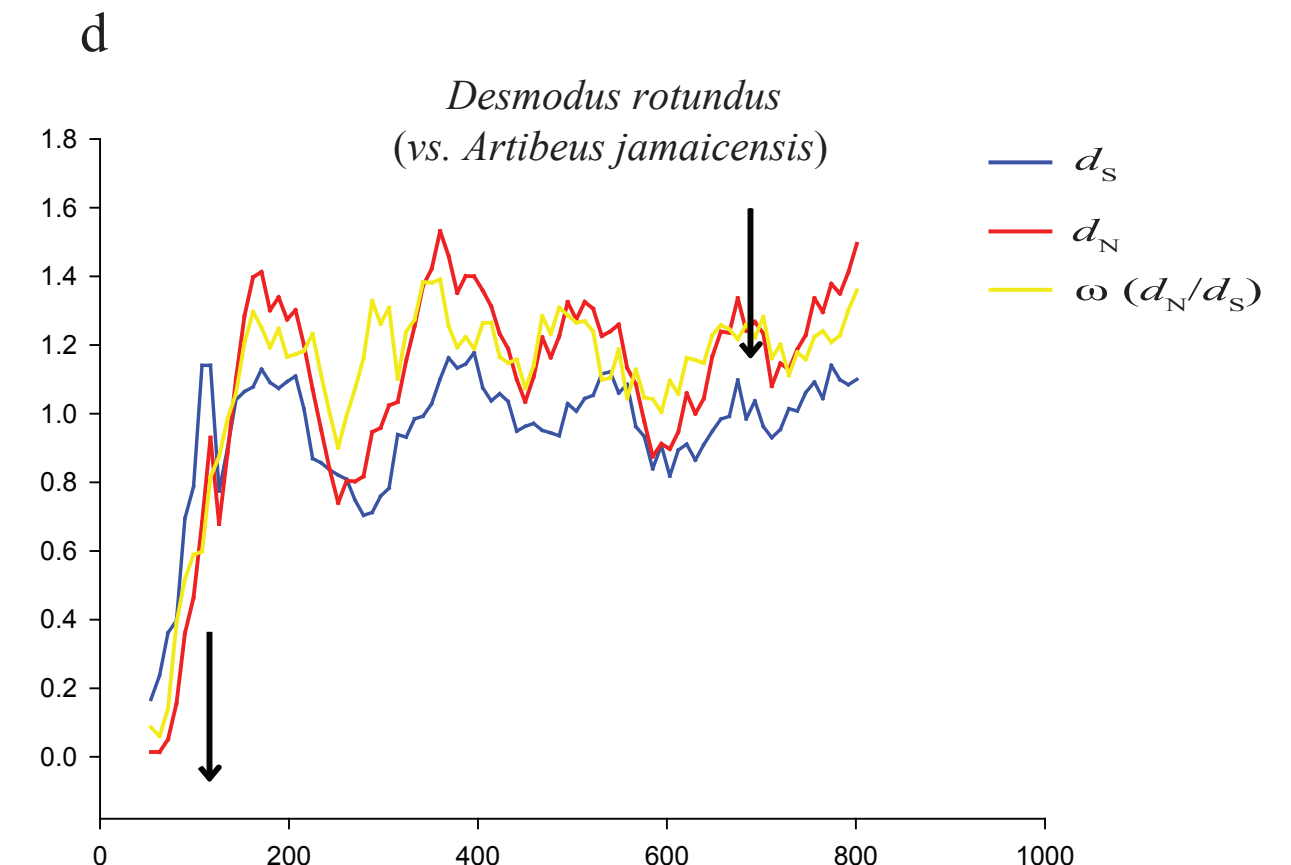
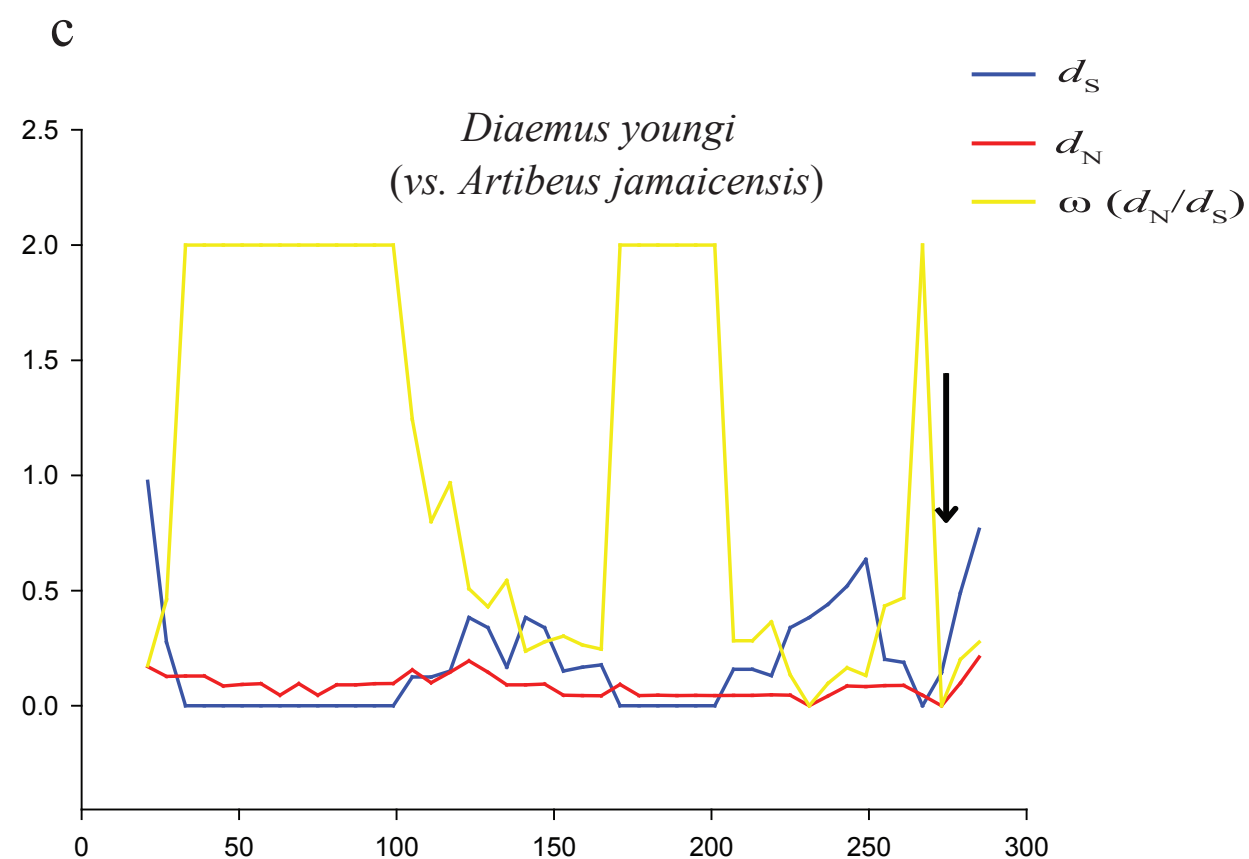
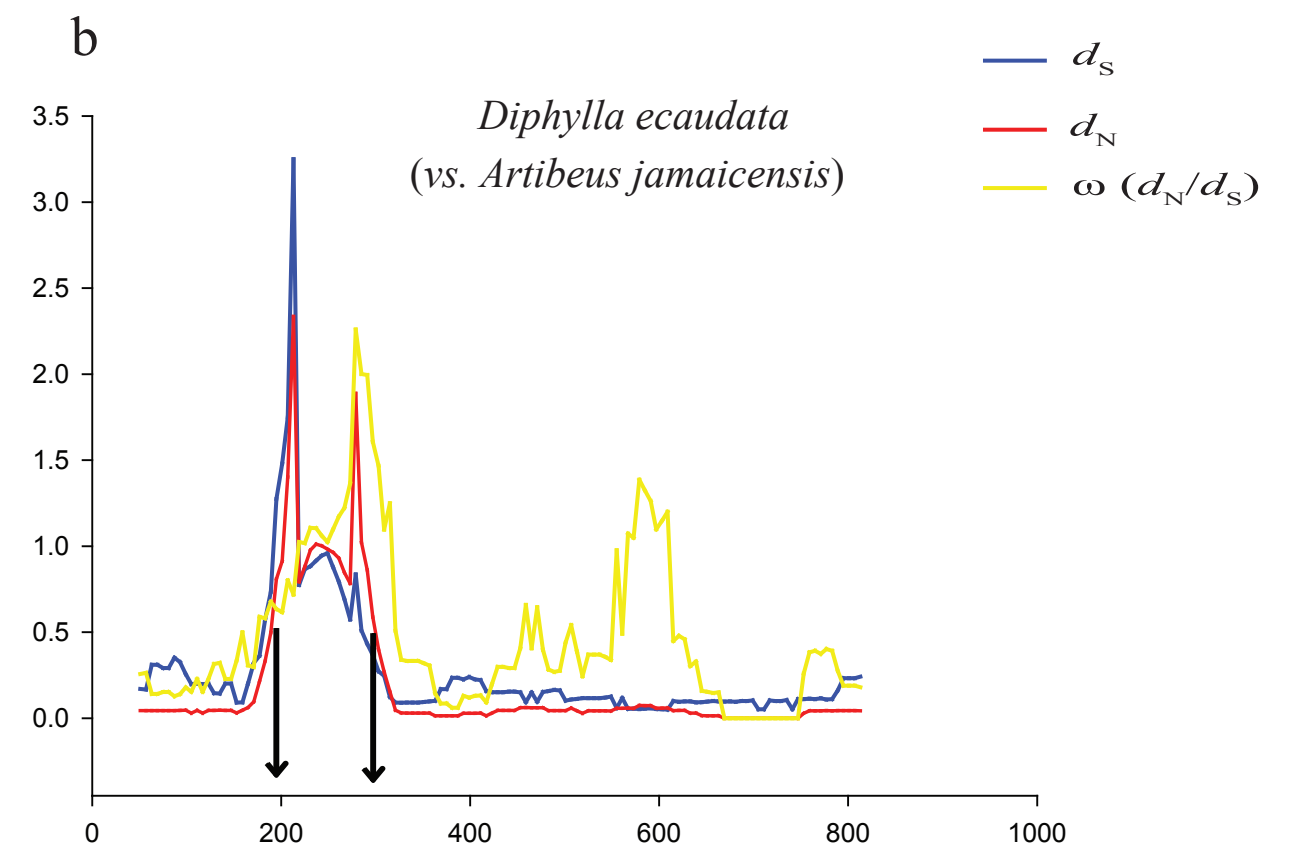
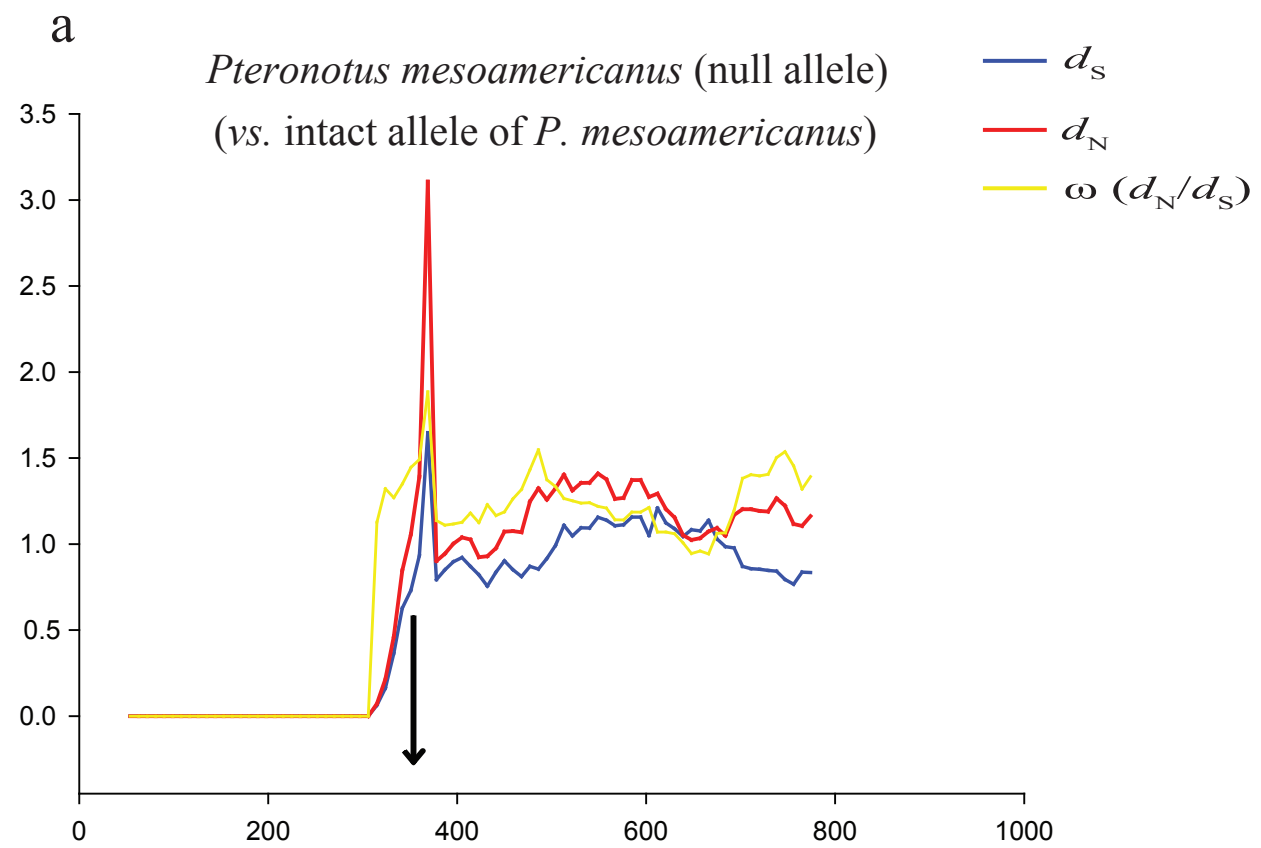
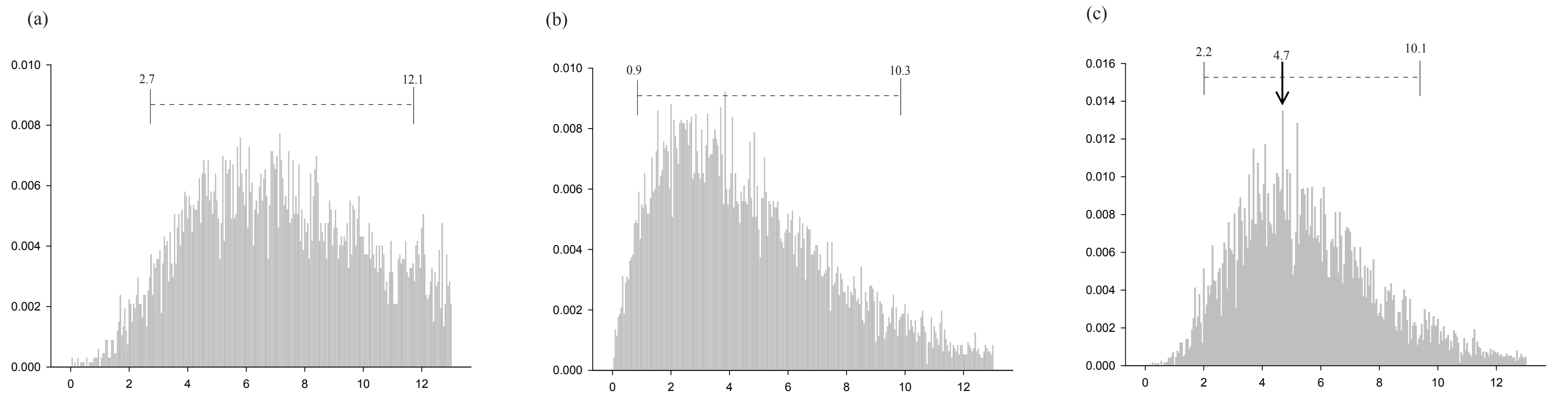


Figure S3. Sliding window analysis of evolutionary changes of the four *SWS1* sequences according to the alignments with their own reading frames. This plot showed the d_S (the synonymous substitution rate) in green line, the d_N (nonsynonymous substitution rate) in red line, and the ω (the ratio of d_N/d_S) in yellow line. The locations of frameshifting indels were indicated by an arrow.

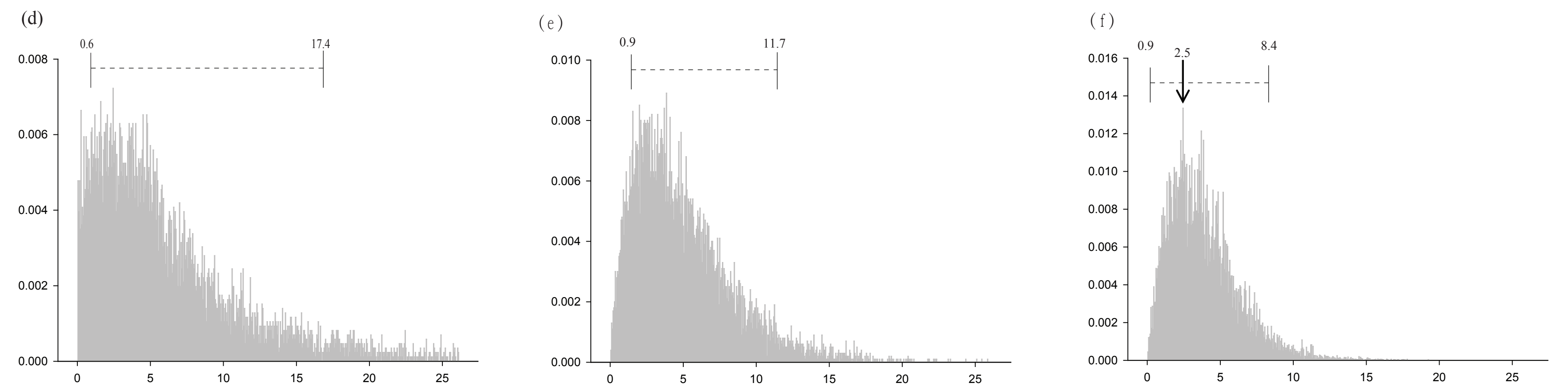
<i>Homo sapiens</i>	ATGAGAAAA	TGTCGGAGGA	AGAGTTTTAT	CTGTTCAAAA	ATATCTCTTC	AGTGGGGCCG	TGGGATGGGC	CTCAGTACCA	CATTGCCCT	90
<i>Desmodus rotundus</i>	ATG-----T	CAGGGGAGGA	GGAGTTTTAT	CTGTTTGAGA	ACATCTCCTC	GGTGGGACCA	TGGGATGGGC	CTCTGTACCA	CATTGCCCT	
<i>Diaemus youngi</i>	??????????	??????????	??????????	??????????	??????????	??????????	??????????	??????????	??????????	
<i>Diphylla ecaudata</i>	ATG-----T	CAGGGGAGGA	GGAGTTTTAT	CTGTTCAAGA	ACATCTCCTT	GGTGGGACCG	TGGGATGGGC	CTCAGTACCA	CATTGCCCTG	
										TM1
	GTCTGGGCCT	TCTACCTCCA	GGCAGCTTTC	ATGGGCACTG	TCTTCCTTAT	AGGGTTCCCA	CTCAATGCCA	TGGTGCTGGT	GGCCACACTG	180
	GTCTGGGCCT	TCCACCTCCA	GGCAGCCTTC	ATGGGCTTTG	TCTTCTTTGC	AGGGATGCC	C-TCAATGCCA	TGGTGCTGGT	GGCCA-----	
	??????????	??????????	??????????	??????????	??????????	??????????	??????????	??????????	??????????	
	GTCTGGGCCT	TCCGCCTCCA	GGCAGCCTTC	ATGGGCTTTG	TCTTCTTTGC	AGGGACACCC	CTCAATGCCA	CGGTGCTGGT	GGCCACACTG	
										TM2
	CGCTACAAAA	AGTTGCGGCA	GCCCCTCAAC	TACATTCTGG	TCAACGTGTC	CTTC-GGAGG	CTTCCTCTC	TGCATCTTCT	CTGTCTTCCC	269
	-----AAA	AGCTGAGGCA	GCCACTCAAC	TACATTTTGA	TCAGTGTGTC	CCTG-GGGGG	CTTCCTCTC	TGCATCTTCT	CTGTGCGCAC	
	??????????	??????????	??????????	??????????	??????????	??????????	??????????	??????????	??????????	
	CGCTACAGAA	AGCTGAGGCG	GCCACTCAAC	TACATTTTGG	TCAATGTGTC	CCTGAGGGGG	CTTCCTCTT	TGCATCTTCT	CTGTCTCCAC	
										TM3
	TGTCTTCGTC	GCCAGCTGTA	ACGGATACTT	CGTCTTCGGT	CGCCATGTTT	GTGCTTTGGA	GGGCTTCCTG	GGCACTGTAG	CAGGTCTGGT	359
	TGTCTTCATT	ACCAGTTGTC	GGGGCTACTT	CACCATCGGG	CGCCGCATGT	GTGCTTTGGA	GGACTTCCTG	GGCTCTACAG	CAGGTCTGGT	
	??????????	??????????	??????????	??????????	??????????	??????????	??????????	??????????	??????????	
	TGTCTTCATC	GCCAGTTGTC	AGGGATACTT	CATCTTCAGC	CGC-ACGTGT	GTGCTTTGGA	GGCCTTCCTG	GGCTCTACAG	CAGGTCTGGT	
										TM4
	TACAGGATGG	TCCTGGCCTT	TGAGCGCTAC	ATTGTCATCT	GTAAGCCCTT	CGGCAACTTC	CGCTTCAGCT	CCAAGCATGC		449
	CACAGGCTGG	TCCTGGCCTT	TGAGCGCTAC	ACTGTCATCT	GCAAACCCTT	TGGCAGCTTC	CGCTTCAGCT	CCAGGCACAC		
	??????????	??????????	??????????	??????????	??????????	??????????	??????????	??????????	??????????	
	CACAGGCTGG	TCCTGGCCTT	TGAGCGATA	ATCGTCATCT	GCAAACCCTT	CGGCAACTTC	CGCTTCAGCT	CCAGGCACGC		
										TM5
	ACTGACGGTG	GTCCTGGCTA	CCTGGACCAT	TGGTATTGGC	GTCTCCATCC	CACCCTTCTT	TGGCTGGAGC	CGGTTTCATCC	CTGAGGGCCT	539
	ACTGTTGGTA	GTCCTGGCCA	CCTGGACCAT	TGGCATCGGC	GTCTCCATCC	CACCCTTCTT	TGGCTGGAGC	CGGTTTCATCC	CCGAGGGCCT	
	??????????	??????????	??????????	??????????	??????????	??????????	??????????	??????????	??????????	
	ACTGATGGTA	GTCCTGACCA	CCTGGACCAT	TGGCATCGGC	GTCTCCATCC	CACTCTTCTT	TGGCTGGAGC	CGGTTTCATCC	CCGAGGGCCT	
										TM6
	GCAGTGTTC	TGTGGCCCTG	ACTGGTACAC	CGTGGGCACC	AAATACCGCA	GCGAGTCCTA	TACGTGGTTC	CTCTTCATCT	TCTGCTTCAT	629
	GCAATGTTCC	TGTGGCCCTG	ACTGGTACAC	TGTGGGCACC	AAATATCACA	GCGAGTACCA	CACCTGGTTC	CTGTTTCATCT	TCTGCTTCAT	
	??????????	??????????	??????????	??????????	AAATATCACA	GTGAGTACTA	CAGCTGGTTC	CTCTTCATCT	TCTGCTTCAT	
	GCAATGTTCC	TGTGGCCCTG	ACTGGTACAC	CGTGGGCACC	AAGTATCGCA	GCGAGTACTA	CACCTGGTTC	CTCTTCATCT	TCTGCTTCAT	
										TM7
	TGTGCCTCTC	TCCCTCATCT	GCTTCTCCTA	CACTCAGCTG	CTGAGGGCCC	TGAAAGCTGT	TGCAGCTCAG	CAGCAGGAGT	CAGCTACGAC	719
	CGTGCATCTT	TCCCTCATCT	GCTTCTCCTA	CTCTCAGCTG	CTGGGGGCGC	TCAGAGCTCT	TGCAGCCCAG	CAGCACGAGT	CGGCTTCGAC	
	CGTGCCTCTT	TCCCTCATCT	GCTTCTTCTA	CTCTAAGCTG	CTGGGGGCGC	TCAAAGCTCT	TGCAGCCCAG	CAGCACAAGT	CGGCTTCGAC	
	CGTGCCTCTC	TCCCTCATCT	GCTTCTGCTA	CTCTCAGCTG	CTGGGGGCGC	TCAGAGCTGT	TGCAGCCCAG	CAGCAGGAGT	CAGCTTCGAC	
										TM8
	CCAGAAGGCT	GAACGGGAGG	TGAGCCGCAT	GGTGGTTGTG	ATGGTAGGAT	CCTTCTGTGT	CTGCTACGTG	CCCTACGCGG	CCTTCGCCAT	809
	CCAGAAGGG-	GAGCGGGAGG	TGAGCCGCAT	GGTGTGGTGT	ATGGTGGGAT	CCTTTTGTCT	CTGTTACGTG	CCCTATGCTG	CCCTGGCCAT	
	CCAGAAGGCC	AAGCGGGAGG	TGAGCCGCAT	GGTGTGGTGT	ATGGTGGGAT	CCTTTTGTCT	CTGTTCCGTG	CCCTATGCTG	CCCTGGCCAT	
	CCAGAAGGCC	GAGCGGGAGG	TGAGCCGCAT	GGTGGTGGTGT	ATGGTGGGAT	CCTTTTGTCT	CTGTTACGTG	CCCTATGCTG	CCCTGGCCAT	
										TM9
	GTACATGGTC	AACAACCGTA	ACCATGGGCT	GGACTTACGG	CTTGTACCA	TTCCTTCATT	CTTCTCCAAG	AGTGCTTGCA	TCTACAATCC	899
	GTATATGGTC	AACCACCGTA	GCCACGGGCT	GGACTTCCAG	CTGGTACCA	TTCCTGC---	CTTCTCCAAG	AGTGCTTGCA	TCTACAATCC	
	GTATATGGTC	AACCACCGTA	GCCACGGGCT	GGACTTCCGG	CTGGTACCA	TTCCTGCCTT	CTTCTCCAAG	??????????	??????????	
	GTACATGGTC	AACAACCGTA	GCCACAGGCT	GGACTTCCGG	CTGGTACCA	TTCCTGCCTT	CTTCTCCAAG	AGTGCTTGCA	TCTACAATCC	
										TM10
	CATCATCTAC	TGCTTCATGA	ATAAGCAGTT	CCAAGCTTGC	ATCATGAAGA	TGGTGTGTGG	GAAGGCCATG	ACAGATGAAT	CCGACACATG	989
	CATCATCTAC	TGCTTCATGA	ATAAGCAGTT	CTGGGCTTGC	ATCACGGAGA	TGGTGTGTGG	GAAGTCCACG	ACAGGTGAGT	CTGACGTGTC	
	??????????	??????????	??????????	??????????	??????????	??????????	??????????	??????????	??????????	
	CATCATCTAC	TGCTTCATGA	ATAAGCAGTG	CCAAGCTTGC	ATCATGGAGA	TGGTGTATGG	GAAGTCCAGG	ACAGAGGAGT	CCGACGTGTC	
										1047
	CAGTCCCAG	AAAACAGAAG	TTTCTACTGT	CTCGTCTACC	CAAGTTGGCC	CCAAGTGA				
	CAGTCCCAG	AGAAGTGAAG	TTTCTACTCT	CTCTTCCAGC	CAAGTTGGCC	CCAGCTAA				
	??????????	??????????	??????????	??????????	??????????	??????????				
	CAGTCCCAG	AGAAGTGAAG	TTTCTACTCT	CTC-CAGC	CAAGTTGGCC	CCAGCTAA				

Figure S4. Detailed alignment of *SWS1* sequences from vampire bats (Subfamily Desmodontinae). Insertions, deletions, and premature stop codons are boxed. Dashes are alignment gaps, question marks represent unamplified nucleotides, and numbers in the right indicate nucleotide positions following the reference sequence (*Homo sapiens*). All seven transmembrane domains are indicated.

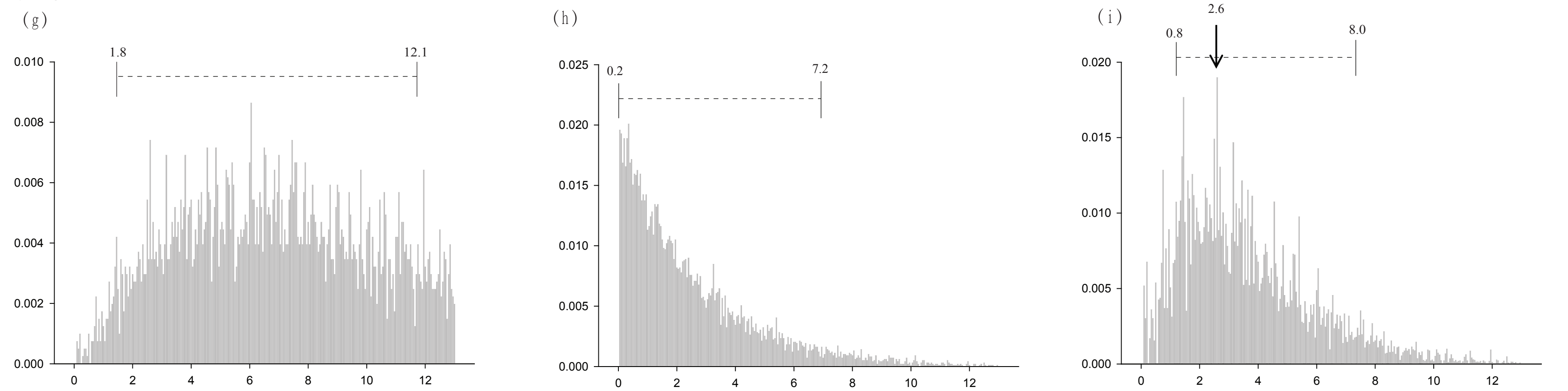
Desmodus rotundus



Diphylla ecaudata



Diaemus youngi



Pteronotus mesoamericanus (null allele)

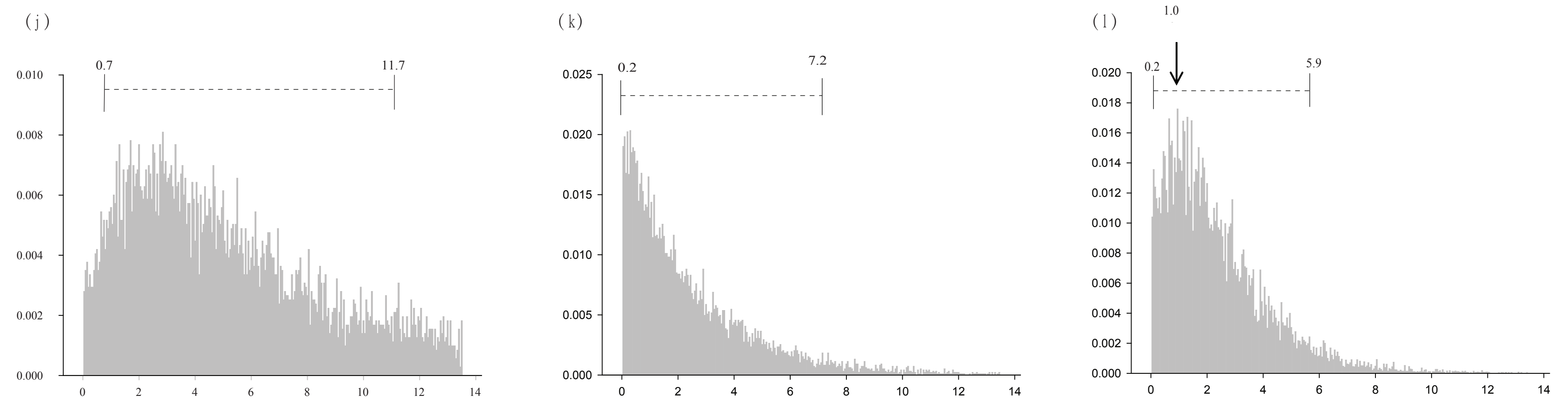


Figure S5. Posterior probability distributions of the time t when the relaxation of functional constraint on *SWS1* started. Posterior probability distribution of t based on the rate of synonymous substitution, the number of ORF-disrupting substitutions and both methods was shown for the common vampire bat (*Desmodus rotundus*) (a-c), the hairy-legged vampire bat (*Diphylla ecaudata*) (d-f), the white-winged vampire bat (*Diaemus youngi*) (g-i), and the *Pteronotus mesoamericanus* (j-l), respectively. The 95% confidence interval of t was indicated on the top of each panel, while the mode of t was shown only in four panels (c, f, i, and l).

A

	46	49	52		86	90	93	97		113	114	116	118
	#	#	#		#	#	#	#		#	#	#	#
<i>Mus musculus</i>													
<i>Artibeus jamaicensis</i>													
<i>Artibeus lituratus</i>													
<i>Carollia perspicillata</i>													
<i>Anoura caudifer</i>													
<i>Brachyphylla cavernarum</i>													
<i>Glossophaga soricina</i>													
<i>Lophostoma silvicolum</i>													
<i>Mesophylla macconnelli</i>													
<i>Phyllonycteris obtusa</i>													
<i>Phyllops falcatus</i>													
<i>Sturnira lilium</i>													
<i>Trachops cirrhosus</i>													
<i>Uroderma bilobatum</i>													
<i>Vampyrum spectrum</i>													
<i>Pteronotus davyi</i>													

B

	180	197		277	285		308
	*	*		*	*		*
<i>Homo sapiens</i>							
<i>Acerodon celebensis</i>							
<i>Harpyionycteris celebensis</i>							
<i>Artibeus jamaicensis</i>							
<i>Chaerephon plicatus</i>							
<i>Cynopterus sphinx</i>							
<i>Hipposideros armiger</i>							
<i>Miniopterus schreibersii</i>							
<i>Myotis ricketti</i>							
<i>Megaderma spasma</i>							
<i>Pipistrellus abramus</i>							
<i>Pteropus giganteus</i>							
<i>Rhinolophus ferrumequinum</i>							
<i>Rousettus leschenaultii</i>							
<i>Taphozous melanopogon</i>							
<i>Desmodus rotundus</i>							

Figure S6. Alignments of amino acid sequences of cone opsins in the New World bats. Asterisks (*) indicate the 11 critical amino acid sites in the SWS1 opsin (a), and number signs (#) indicate the five key sites in the M/LWS opsin (b).

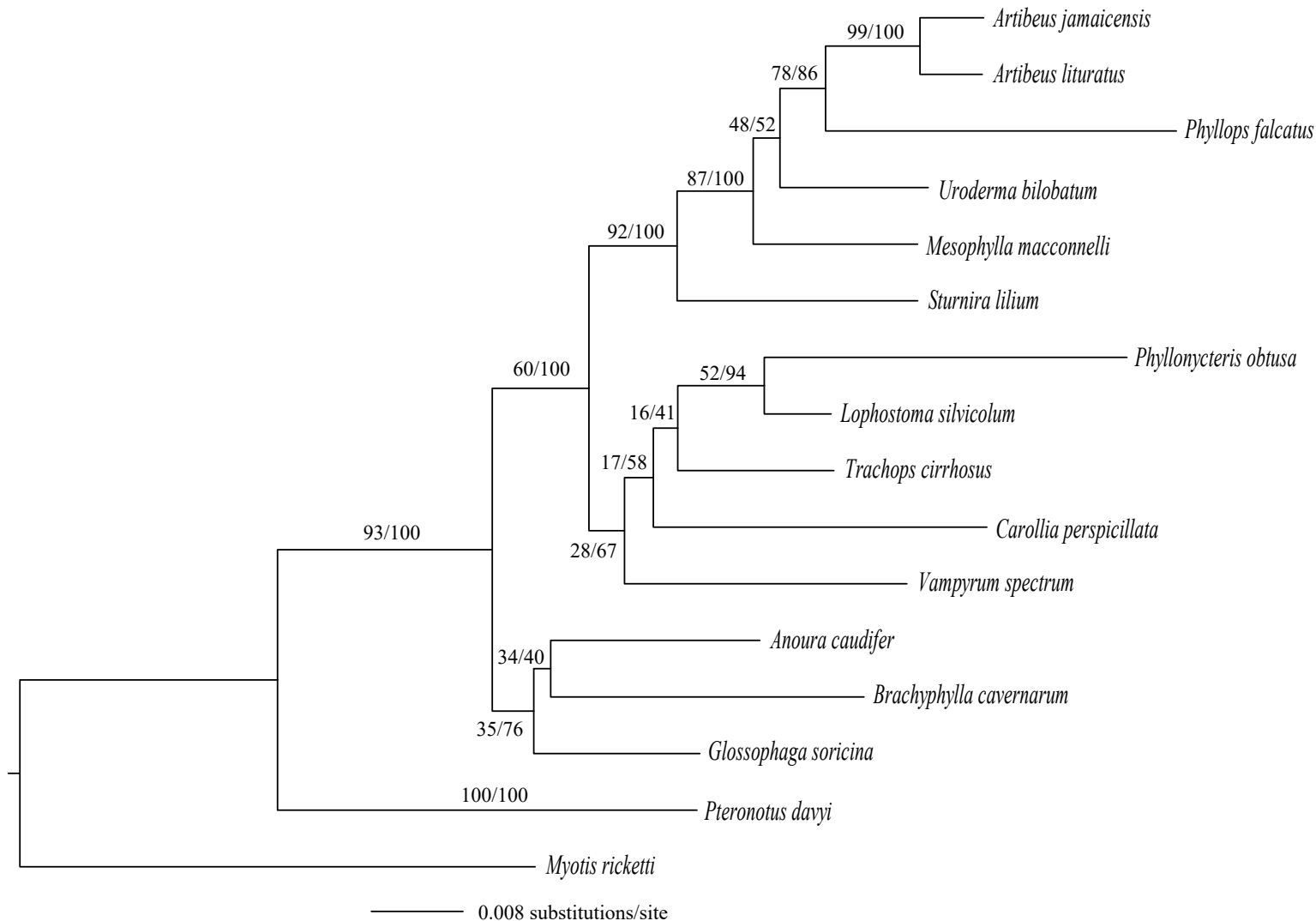


Figure S7. The maximum likelihood tree for the *SWS1* dataset of the New World bats. Numbers at the nodes are the ML bootstrap values/Bayesian posterior probabilities, shown as percentages.